Multinucleon removal induced by 80-MeV ^{3}He†

P. P. Singh, M. Sadler, and A. Nadasen
Indiana University Cyclotron Facility, Indiana University, Bloomington, Indiana 47401

L. A. Beach and C. R. Gossett
Naval Research Laboratory, Washington, D. C. 20375

(Received 21 January 1976)

γ ray spectra were observed following the bombardment of thin ^{24}Mg, ^{26}Mg, ^{27}Al, Fe, ^{58}Ni, and ^{64}Zn targets with an 80-MeV ^{3}He beam. Product nuclei were identified using their characteristic γ rays. Qualitative features of the results can be understood in terms of the evaporation process preceded by pre-equilibrium emission. Results with ^{3}He are similar to those obtained with comparable energy proton and pion beams. Systematics are discussed.

[NUCLEAR REACTIONS: (^{3}He,$xnypz\alpha\gamma$) with ^{24}Mg, ^{26}Mg, ^{27}Al, Fe, ^{58}Ni, and ^{64}Zn targets. Measured γ-ray spectra. Deduced relative cross sections for production of final nuclei following multinucleon removal.]

Recently studies of multinucleon removal following interactions of stopped, slow and fast pions (π^+ and π^-), stopped kaons, and intermediate energy protons with targets of mass between 20 and 90 have been reported.[1-7] We present here results with 80-MeV ^{3}He projectiles on ^{24}Mg, ^{26}Mg, ^{27}Al, Fe, ^{58}Ni, and ^{64}Zn targets. These measurements were made to see if the characteristics of the multinucleon removal with complex projectiles are any different from those with protons and pions.

The ^{3}He beam from the Naval Research cyclotron was used to bombard isotopically rich (except for iron) targets of 1–5 mg/cm^2 in thickness. The γ rays were detected with a Ge(Li) detector, placed about 3 cm from the targets at 90° to the beam, with an overall energy resolution of 3 keV. The γ-ray events were time gated and were recorded in prompt and delayed modes. The prompt spectrum covered a time span of 30 nsec around the beam bursts (of 2–4-nsec duration), and the delayed spectrum corresponded to events produced in the time range of 30–90 nsec following every beam burst. Typical spectra for the ^{58}Ni target are shown in Fig. 1. Generally about 60 and 25 γ-ray peaks were observed in prompt and delayed spectra, respectively, with each target. The energies of the observed γ rays were used in conjunction with the known γ-decay modes of nuclei in the mass range of 12–70 to assign them to a particular product nucleus. After correcting for detector geometry and efficiency (measured using calibrated radioactive sources) and assuming an isotropic angular distribution for the γ rays, the observed prompt yield of each γ ray was con-

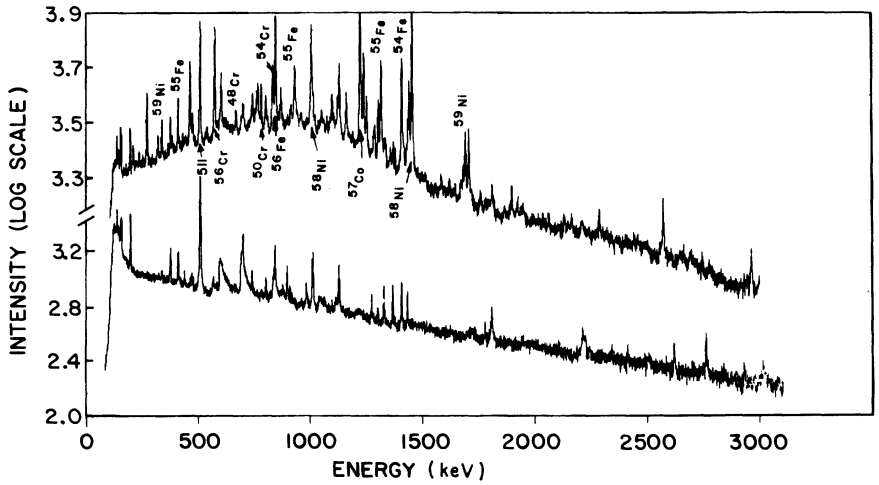

FIG. 1. The prompt (top) and delayed (bottom) γ-ray spectra obtained with ^{58}Ni target.

verted to a relative production cross section for each final nucleus. The delayed strength of each γ ray assigned to a particular nucleus was used to determine the production cross section of adjoining nuclei undergoing β decay to the former. Since the beam current, typically ~0.2 nA, could not be measured accurately the production cross sections in Tables I and II are relative.

The following are the main characteristics of the ^{3}He induced production. (a) Irrespective of the target mass the product nuclides lie close to the line of stability. (b) The production of naturally stable nuclei constitutes about 80 and 40% of the total observed cross section with light (^{24}Mg, ^{26}Mg, and ^{27}Al) and medium mass (Fe, ^{58}Ni, and ^{62}Zn) targets, respectively. (c) The nuclei which are produced with cross sections $\gtrsim$5% of the total correspond to $1n$, $1p$, $1n1p$, $2n1p$, $2p1n$, $2p2n$, and $2p3n$ removal from the target. With the ^{27}Al target noticeable removal of $3p2n$, $3p3n$, and $3p4n$ is also observed. With ^{64}Zn, target removal of $4p5n$,

TABLE I. Production cross sections. The observed and the calculated (in parentheses) cross sections, in units of mb, are relative. The total cross section, in all cases have been normalized to 1 b. The calculations are the results of the evaporation plus the pre-equilibrium model.

Product Nuclei	Target ^{27}Al	^{26}Mg	^{24}Mg
^{28}Si	25[a] (24)	(0)	
^{27}Al	129 (93)	24 (30)	
^{26}Al	69(110)	21 (49)	2 (2)
^{25}Al	(22)	(0)	13 (15)
^{27}Mg	(1)	21 (1)	
^{26}Mg	144 (86)	270 (59)	
^{25}Mg	39(164)	73(156)	12 (21)
^{24}Mg	185 (52)	157 (82)	364 (93)
^{23}Mg	24 (20)	13 (6)	77 (54)
^{22}Mg	(2)	(1)	2 (7)
^{25}Na	(8)	7 (15)	
^{24}Na	8 (33)	7 (87)	1 (25)
^{23}Na	158(106)	124 (75)	134(153)
^{22}Na	69 (80)	57 (70)	78(128)
^{21}Na	(3)	3 (12)	20 (30)
^{22}Ne	42 (39)	84 (47)	23 (32)
^{21}Ne	53 (22)	92(109)	65 (57)
^{20}Ne	44 (26)	17 (16)	162(110)
^{19}Ne	(6)	(5)	5 (39)
^{20}F	(5)	6 (6)	4 (15)
^{19}F	10[a] (32)	9[a] (4)	12[a] (79)
^{18}F	(5)	(45)	15 (36)
^{17}F	(0)	(0)	≤4 (34)
^{18}O	(0)	≤7 (16)	≤2 (2)
^{17}O	(0)	6[a] (16)	5[a] (40)

[a] These values may be overestimated by as much as 50%.

TABLE II. Production cross sections. The observed and the calculated (in parentheses) cross sections, in units of mb, are relative. The total cross section, in all cases have been normalized to 1 b. The calculations are the results of the evaporation plus the pre-equilibrium model.

Product Nuclei	Targets ^{64}Zn	^{58}Ni	^{56}Fe
^{64}Ga	27 (8)		
^{64}Zn	196 (73)		
^{63}Zn	82 (22)		
^{62}Zn	7 (8)		
^{61}Zn	23 (1)	(0)	
^{63}Cu	53 (59)		
^{61}Cu	34 (55)		
^{60}Cu	10 (17)	(12)	
^{59}Cu	5 (2)	8 (19)	
^{62}Ni	64 (10)		
^{60}Ni	92(122)		
^{59}Ni	70(139)	95 (72)	(0)
^{58}Ni	23 (74)	133(110)	(8)
^{57}Ni	17 (10)	13 (47)	(15)
^{59}Co	13 (12)		
^{58}Co	(31)	33 (24)	(21)
^{57}Co	21 (29)	171 (79)	94 (94)
^{56}Co	(39)	89 (89)	60(106)
^{55}Co	(15)	3 (82)	0 (48)
^{54}Co	4 (0)	11 (6)	8 (2)
^{58}Fe	10 (0)		
^{57}Fe	15 (1)	(1)	9 (7)
^{56}Fe	12 (9)	84 (13)	145 (51)
^{55}Fe	90 (18)	132 (46)	213 (92)
^{54}Fe	(2)	36(117)	87(117)
^{53}Fe	46 (1)	22 (36)	73 (12)
^{57}Mn	6 (0)		
^{56}Mn	15 (0)	6 (0)	36 (1)
^{53}Mn	2 (5)	16(122)	16(115)
^{52}Mn	2 (1)	6 (44)	(37)
^{51}Mn	(0)	3 (2)	8 (11)
^{50}Mn	(0)	1 (1)	0 (0)
^{54}Cr	(0)	40 (0)	(0)
^{53}Cr	(0)	11 (0)	(2)
^{52}Cr	(1)	15 (35)	50 (58)
^{51}Cr	25[a] (0)	(15)	86 (93)
^{50}Cr	(0)	15 (9)	41 (23)
^{49}Cr	(0)	(0)	39[a] (0)
^{48}Cr	(0)	10 (0)	(0)
^{52}V	(0)	(0)	17 (0)
^{51}V	11[a] (0)	9 (0)	(11)
^{50}V	(0)	(3)	3 (29)
^{51}Ti	27[a] (0)	9 (0)	(0)
^{50}Ti	(0)	4 (0)	0 (0)
^{49}Ti	(0)	(0)	5 (0)
^{48}Ti	(0)	6 (0)	13 (4)
^{45}Ti	(0)	5 (0)	(0)
^{48}Sc	(0)	6[a] (0)	(0)
^{45}Sc	(0)	9[a] (0)	(0)

[a] Same as in Table I.

$4p7n$, and $6p7n$ is observed with significant, ~3% of the total, cross section. With 80-MeV ^{3}He projectiles removal of up to six nucleons is energetically possible since the Q value for six nucleon removal is about 70 MeV. Therefore it is very likely that production of nuclides requiring removal of more than six nucleons involves emission of one or more clusters such as d, t, τ, or α, as the case may be.

The production cross sections as a function of the number of nucleons removed from the target are plotted (histograms) in Fig. 2 for ^{27}Al, ^{64}Zn, and ^{58}Ni targets. For all cases investigated, except for ^{64}Zn, the distribution is a broad peak, somewhat asymmetric towards large nucleon removal, centered about three nucleons removed from the targets. The ^{64}Zn distribution has a tail extending from 6 to 13 nucleon removal. The predictions of the evaporation model[8] with and without pre-equilibrium emission are indicated in Fig. 2. The evaporation model (dashed-dot curves), besides giving a rather peaked distribution, drastically underestimates the removal of a few nucleons. With pre-equilibrium included (solid curves) the calculations are qualitatively able to account for the observed pattern for all targets, and even a broader distribution is predicted for ^{64}Zn. If α emission is not allowed in the evaporation plus pre-equilibrium calculations (dotted curves) cross sections for five or more nucleons removal is noticeably underestimated. Though one will need more sophisticated model calculations to obtain quantitative agreement with the observations, nuclide by nuclide, it is clear that pre-equilibrium nucleon emission followed by evaporation of individual nucleons and clusters is essentially the correct picture to explain the qualitative trends in the observed results.

The above pattern of production with ^{3}He appears to be similar to that found for other types of projectiles of comparable energy. The dependence on particle type and energy of two average indicators of the nucleon removal is presented in Table III. (a) The mean number of nucleons removed $\langle \Delta A \rangle$ with the 80-MeV ^{3}He projectile is ~3.3 for all targets. Almost the same value is found with other projectiles of comparable energy. Since a large number of nucleon removal from the target mass is produced by the evaporation process, in contrast to the pre-equilibrium process (see Fig. 2), a small increase in $\langle \Delta A \rangle$ in going from 100- to 200-MeV protons indicates that at higher energies pre-equilibrium is more important and relatively small additional energy is deposited in the compound nucleus. The invariance of $\langle \Delta A \rangle$ with pion energy implies that evaporation ensues only after pions have been absorbed. The difference in $\langle \Delta A \rangle$ for 200-MeV proton and pion results indicates that the average compound nuclear excitation energy with protons is less than that (~150 MeV) resulting from the absorption of pions.

(b) The ratio $\langle \Delta N \rangle / \langle \Delta Z \rangle$ appears to be independent of the projectile type and its energy. Since the observed product nuclei lie near the line of stability, their $N-Z$ is similar to that of the target nucleus and thus one would expect this ratio to be close to unity as observed. In particular, the $N-Z$ for $^{58}_{28}$Ni is 2, but that of the nuclei produced

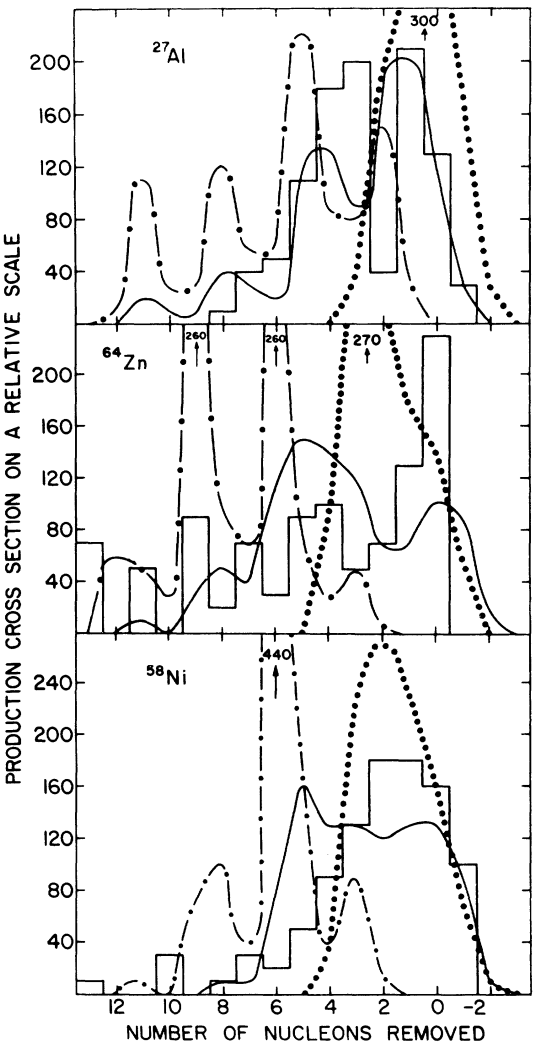

FIG. 2. The production cross sections as a function of number of nucleon removed from the target mass. The histograms represent measurements. The dashed-dot curves are the results of the evaporation model and the solid curves are those of the evaporation plus pre-equilibrium model. The dotted curves represent the results of the calculations when α emission is inhibited from the second model.

TABLE III. Average nucleon removal from various targets by different projectiles. The 190-MeV p, 100-MeV π^+, and 100-MeV p results are from Refs. 6, 4, and 5, respectively. The other results are from Ref. 7.

Target	^{24}Mg	^{26}Mg	^{27}Al			Fe	^{58}Ni						^{64}Zn
Energy (MeV)	80	80	80	190	100	80	80	100	200	100	200	220	80
Projectile	^{3}He	^{3}He	^{3}He	p	π^+	^{3}He	^{3}He	p	p	π^+	π^+	π^-	^{3}He
$\langle\Delta A\rangle$ [a]	>2.8	3.3	3.4	3.3	3.4 [d]	3.2	3.2	3.3	4.1	5.2	5.4	5.4	4.4
Theory [b]	3.6	3.5	3.2			3.2							4.6
$\langle\Delta N\rangle/\langle\Delta Z\rangle$ [c]	1.0	1.4	1.3	1.2	1.17	1.0	0.78	0.77	0.7	0.8	0.76	0.76	1.1
Theory [b]	1.0	1.3	1.1			1.2	0.95						1.4

[a] The target mass number minus the cross section-weighted average mass number of product nuclides, not counting inelastic scattering.

[b] Predictions with evaporation plus pre-equilibrium model.

[c] The ratio of the average number of neutrons and protons removed computed as in a.

[d] Pions not stopped in the target.[4]

with this target is in the range of 3–4. Therefore, on an average, in this case one will have to emit more protons than neutrons to stay in the vicinity of the line of stability, and so a value smaller than unity should be expected. The $N-Z$ of $^{56}_{26}$Fe and $^{64}_{30}$Zn on the other hand is 4 and therefore the ratio should be a little greater than unity as seems to be the case. Because different projectiles of various energies lead to the same product nuclei ($\langle\Delta A\rangle$ not very different) with a given target, invariance of $\langle\Delta N\rangle/\langle\Delta Z\rangle$ on projectile type and its energy is expected from this viewpoint. It is interesting to note (Table III) that the evaporation model with pre-equilibrium is able to reproduce the observed trends in values of $\langle\Delta A\rangle$ and $\langle\Delta N\rangle/\langle\Delta Z\rangle$.

In summary, the nucleon removal with 80-MeV ^{3}He projectiles is found to be similar to that observed with other projectiles. An interaction mechanism involving evaporation preceded by pre-equilibrium emission is able to explain the qualitative trends in the observed cross sections but fails to give quantitative agreement for individual nuclides. Considerable improvements in model calculations are needed.

We wish to acknowledge helpful discussions with Professor M. Blann regarding the results of the codes ALICE and HYBRID.

†Work supported in part by the National Science Foundation.

[1]P. D. Barnes *et al.*, Phys. Rev. Lett. 29, 230 (1972).
[2]H. E. Jackson *et al.*, Phys. Rev. Lett. 31, 1352 (1973).
[3]V. G. Lind *et al.*, Phys. Rev. Lett. 32, 479 (1974).
[4]D. Ashery *et al.*, Phys. Rev. Lett. 32, 943 (1974).
[5]C. C. Chang *et al.*, Phys. Rev. Lett. 33, 1493 (1974).
[5]C. C. Chang, N. S. Wall, and Z. Fraenkel, Phys. Rev. Lett. 33, 1493 (1974).
[6]O. Artun *et al.*, Phys. Rev. Lett. 35, 773 (1975).
[7]H. E. Jackson *et al.*, Phys. Rev. Lett. 35, 641 (1975).
[8]These calculations were performed using ALICE and HYBRID codes written by M. Blann and F. Plasil. M. Blann, Ann. Rev. Nucl. Phys., 25, 123 (1975).